McCoy, S., & Caughey, W. S. (1970) *Biochemistry 9*, 2387.
Spaulding, L. D., Chang, R. C. C., Yu, N.-T., & Felton, R. H. (1975) *J. Am. Chem. Soc. 97*, 2517.
Spiro, T. G. & Strekas, T. C. (1974) *J. Am. Chem. Soc. 96*, 338.
Spiro, T. G., Stong, J. D., & Stein, P. (1979) *J. Am. Chem. Soc. 101*, 2648.
Stryer, L., Kendrew, J. C., & Watson, H. C. (1964) *J. Mol. Biol. 8*, 96.
Wilson, E. B., Jr., Decius, J. C., & Cross, P. C. (1955) *Molecular Vibrations*, McGraw-Hill, New York.
Wright, P. G., Stein, P., Burke, J. M., & Spiro, T. G. (1979) *J. Am. Chem. Soc. 101*, 3531.
Yu, N.-T., & Srivastava, R. B. (1980) *J. Raman Spectrosc. 9*, 166.
Yu, N.-T., & Tsubaki, M. (1980) *Biochemistry 19*, 4647.
Zerner, M., Gouterman, M., & Kobayashi, H. (1966) *Theor. Chim. Acta 6*, 363.

Insights into Heme Structure from Soret Excitation Raman Spectroscopy†

Patricia M. Callahan and Gerald T. Babcock*

ABSTRACT: Laser lines in resonance with the Soret band optical transitions of several heme proteins and heme model compounds have been used to obtain Raman spectra of these species. Correlations between the observed frequency of a polarized mode in the 1560–1600-cm^{-1} region and the heme iron spin and coordination geometry have been developed. The position of this band is also a function of the pattern of porphyrin pyrrole ring β-carbon substitution, and therefore structural information can be extracted from the Raman data only after this dependence has been taken into account. Quantitative correlations between the frequency of this band and the porphyrin core size are presented for three commonly occurring classes of heme compounds: (a) protoheme derivatives, (b) iron porphyrins in which all ring positions are saturated, and (c) heme *a* species. A polarized mode in the 1470–1510-cm^{-1} region is also consistently enhanced upon Soret excitation of these compounds, but is relatively insensitive to peripheral substituents, and can be used in conjunction with the polarized mode described above to assign heme geometries. In the frequency region above 1600 cm^{-1}, a vibration is observed which also responds to changes in porphyrin geometry. However, this band is sometimes obscured by vibrations of unsaturated β-carbon substituents, particularly in the case of protoheme derivatives. The normal coordinate analysis developed by Abe and co-workers [Abe, M., Kitagawa, T., & Kyogoku, Y. (1978) *J. Chem. Phys. 69*, 4526–4534] is used to rationalize the dependence of the various modes on porphyrin geometry and peripheral substitution.

The geometry of the porphyrin macrocycle in hemes and heme proteins is reflected in the frequency positions of several vibrational bands observed by resonance Raman spectroscopy (Spiro, 1974; Felton & Yu, 1978; Kitagawa et al., 1978; Rousseau et al., 1979). One of the most useful empirical correlations between heme structure and Raman frequency has been developed by Spaulding et al. (1975), who showed that an inverse relationship exists between the frequency of an anomalously polarized mode in the 1550–1610-cm^{-1} region and C_t–N, the distance from the center of the porphyrin to the pyrrole nitrogens. This was later confirmed and extended (Huong & Pommier, 1977; Scholler & Hoffman, 1979; Spiro et al., 1979), and plots of Raman frequency vs. porphyrin core size (C_t–N) for the ap[1] mode (denoted band IV) as well as for a polarized mode in the 1470–1510-cm^{-1} region (band II) and for a depolarized mode in the 1600–1650-cm^{-1} region (band V) could be fit by an empirical equation of the form

$$\bar{\nu}_i = K_i(A_i - d) \text{ cm}^{-1} \quad (1)$$

where $\bar{\nu}_i$ is the frequency of the vibration under consideration, d the C_t–N distance, and K_i and A_i are adjustable parameters specific to the ith vibration. Equation 1 has thus far been established for the three vibrational bands indicated above, all of which have appreciable methine bridge bond stretching character (Spiro et al., 1979). As a consequence, the correlations indicated by eq 1 are relatively insensitive to the nature of the pyrrole β-carbon substituents, provided that these are linked by C_β–C_s bonds. However, replacement of the hydrogen at the methine bridge carbon by, for example, phenyl groups or deuterium, causes shifts in these bands unrelated to core size change, and eq 1 is no longer applicable. In addition, bands II and V are also somewhat sensitive to the nature of the axial ligands and shift to higher frequency as the π acceptor character of the ligands is increased.

With the establishment of sound correlations between porphyrin core size and Raman frequency, it has become possible to interpret scattering data to determine both spin state and iron coordination number for several heme proteins (Spiro et al., 1979; Sievers et al., 1979). However, the research which has been done thus far to link porphyrin core size and Raman vibrational frequencies has been carried out with α,β excitation. Under these conditions Herzberg–Teller scattering dominates, and, for a porphyrin of D_{4h} symmetry, enhancement of modes of A_{2g}, B_{1g}, and B_{2g} symmetry is strong whereas A_{1g} modes are weak or absent (Friedman & Hochstrasser, 1973; Felton & Yu, 1978; Rousseau et al., 1979). For Soret excitation, on the other hand, scattering occurs by a Franck–Condon mechanism, and the opposite pattern of vibrational enhancement is observed: polarized modes dominate the spectrum, and anomalously polarized and depolarized lines are weak. Additionally, depolarized modes can acquire A-term intensity

† From the Department of Chemistry, Michigan State University, East Lansing, Michigan 48824. *Received July 16, 1980.* This investigation was supported by National Institutes of Health Grant No. GM25480.

[1] Abbreviations used: ap, anomalously polarized; Me_2SO, dimethyl sulfoxide; dp, depolarized; Hepes, *N*-(2-hydroxyethyl)piperazine-*N*′-2-ethanesulfonic acid; HRP, horseradish peroxidase; NMeIm, *N*-methylimidazole; OEP, octaethylporphyrin; p, polarized; PPIX DME, protoporphyrin IX dimethyl ester; $NaDodSO_4$, sodium dodecyl sulfate.

0006-2960/81/0420-0952$01.00/0

as a result of the dynamic Jahn-Teller effect (Shelnutt et al., 1977). Thus the vibrations observed upon Soret excitation of hemes and heme proteins are, in general, distinct from those enhanced by α,β excitation, and the empirical correlation between core size and Raman frequency described above for Herzberg–Teller active modes may not necessarily apply to the Franck–Condon vibrations.

Sporadic reports have appeared in the literature which relate the frequency of a polarized mode in the 1560–1600-cm^{-1} region, observed with Soret excitation, to heme iron spin state. For example, Yamamoto et al. (1973) reported such a correlation for hemoglobin and myoglobin compounds, Remba et al. (1979) reported analogous data for chloroperoxidase, and Babcock & Salmeen (1979) tabulated the frequency of this band as a function of heme *a* iron spin state. However, a systematic study of this phenomenon has not yet appeared. In the research reported here, we have investigated the Raman spectra of a number of heme model compounds and heme proteins[2] and have established an empirical correlation between the frequencies of the observed modes, the porphyrin core size, and the pattern of β-carbon peripheral substituents. A preliminary account of this work has been presented (Babcock et al., 1980). In the following paper (Babcock et al., 1981) we apply this correlation to the interpretation of Soret excitation Raman spectra of cytochrome oxidase and a number of its inhibitor complexes.

Materials and Methods

Horse heart myoglobin was obtained from Sigma Chemical Co.; complete formation of the met form was achieved by oxidation with excess potassium ferricyanide and subsequent passage through a Sephadex G-25 column. Human hemoglobin from P-L Biochemicals was treated in an analogous fashion. The fluoride complexes of these compounds were prepared by diluting the concentrated stock solutions with 1 M solutions of sodium fluoride in 0.1 M Hepes buffer, pH 6.9; azide complexes were prepared in an analogous manner by using 500 mM solutions of sodium azide in 0.1 M Hepes buffer, pH 7.4. Horseradish peroxidase (Type VI, Sigma) was used as received and dissolved in 0.1 M Hepes buffer, pH 7.4. Its fluoro and cyano complexes were prepared by diluting the HRP stock solutions with neutral, concentrated stock solutions of NaF and NaCN in 0.1 M Hepes, pH 7.4. Cytochrome *c* (Type VI, Sigma) was dissolved in 0.1 M Hepes, pH 7.4, treated with a slight excess of potassium ferricyanide to ensure complete oxidation, and passed through a Sephadex G-25 column to remove the oxidizing agent.

The chloride complex of heme *a* was isolated from purified beef heart cytochrome oxidase as described previously (Babcock et al., 1976). Low-spin ferric heme *a* complexes in 0.1 M phosphate buffer (pH 7.4)–2% $NaDodSO_4$ and in methylene chloride were prepared by addition of 0.7 M *N*-methylimidazole. Six-coordinate high-spin ferric heme *a* $(Me_2SO)_2$ was obtained by a procedure analogous to that used in the preparation of high-spin six-coordinate iron(III) octaethylporphyrin and iron(III) tetraphenylporphyrin (Dolphin et al., 1977; Zobrist & LaMar, 1978; Spiro et al., 1979): heme a^{3+} perchlorate was prepared from a methylene chloride solution of the heme a^{3+} chloride complex by addition of solid anhydrous $AgClO_4$; following filtration, sufficient Me_2SO was added to ensure formation of the six-coordinate high-spin complex as judged by changes in the optical spectrum (see Figure 1). All complexes obeyed Beer's law in the concentration range used in the experiments described below.

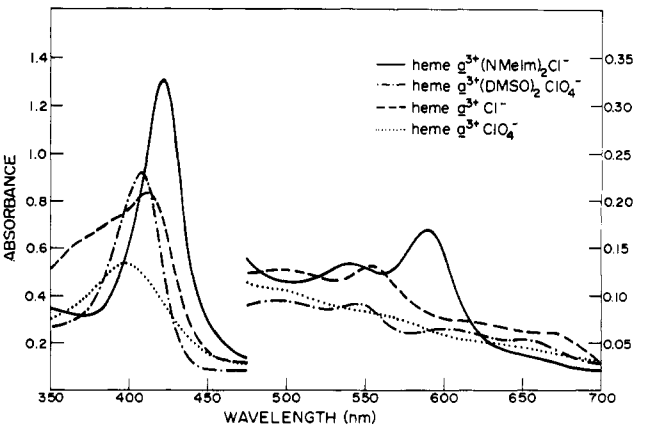

FIGURE 1: Optical absorption spectra of several ferric heme *a* species used in the present study. The heme *a* concentration was ~13 μM for all samples; the solvent was methylene chloride.

Hemin chloride was obtained from Sigma, and the low-spin ferric bis(*N*-methylimidazole) complex was prepared by addition of 0.7 M *N*-methylimidazole to a solution of the heme in 0.1 M sodium phosphate and 2% $NaDodSO_4$, pH 7.4. Protoporphyrin IX dimethyl ester was obtained from Sigma, and the iron insertion was carried out as described by Lemberg et al. (1955) to form the iron(III) protoheme dimethyl ester chloride compound. Iron(III) etioporphyrin I chloride and iron(III) octaethylporphyrin chloride were the kind gifts of Professor C. K. Chang. Preparation of the six-coordinate high- and low-spin species was achieved as described above for the heme a^{3+} complexes. During the preparation of the various derivatives, the optical absorption spectra were monitored to ensure complete formation of the species of interest.

Raman spectra were recorded by using the 406.7- and 413.1-nm lines of a Spectra Physics 164-11 krypton laser and the Spex 1401 Ramalog spectrometer described previously (Ondrias & Babcock, 1980).[3] The power incident on the sample was typically 20 mW. A jacketed cell holder and cold, flowing N_2 gas were used to maintain protein sample temperatures near 4 °C. The sample was contained in a 5 mm path length optical cuvette and 90° scattering was observed by using bottom illumination of the cuvette. Raman spectra for the model complexes were obtained at room temperature by using a spinning sample cell constructed at Michigan State University. The concentration of both protein and heme model compound samples was adjusted to give an absorbance between 1 and 2 at the excitation frequency; typical concentrations required to achieve this were between 10 and 20 μM. For both the protein samples and the heme model complexes, optical spectra were recorded before and after the Raman experiment to monitor sample integrity. No precipitate formed in the samples during illumination, and lower laser powers could reproduce the spectra reported here. Other experimental conditions are given in the tables and figure legends.

Results

Protoheme Species. Soret excitation Raman spectra of several protoheme-containing species are presented in Figures 2 and 3. These have been selected to represent the commonly

[2] We have focused here primarily on the oxidized forms of the various heme compounds. In a future work (I. Salmeen and G. T. Babcock, unpublished experiments) we will present data on reduced species with a particular emphasis on cytochrome oxidase.

[3] The spectrometer used in an earlier study on heme *a* (Babcock & Salmeen, 1979) was miscalibrated by ~7 cm^{-1} in the 1500–1700-cm^{-1} region. This has been corrected in the present study by carrying out a benzene calibration prior to each series of experiments.

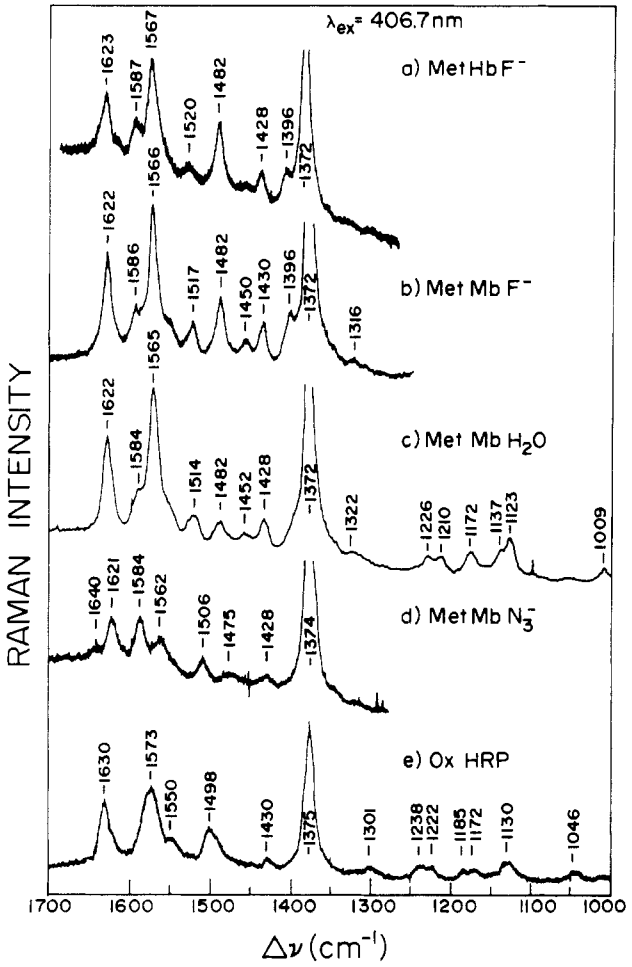

FIGURE 2: Resonance Raman spectra of several protoheme-containing heme proteins. Instrumental conditions: resolution, 6 cm^{-1}; time constant, 1 s; scan rate, 50 cm^{-1}/min. The buffer composition and ligand concentrations are given under Materials and Methods.

encountered combinations of spin state and iron coordination:[4] (a) six-coordinate low-spin (Figure 2d; Figure 3c,d); (b) six-coordinate high-spin (Figure 2a,b,c; Figure 3b); (c) five-coordinate high-spin (Figure 2e; Figure 3a). The spectrum of oxidized HRP (Figure 2e) is similar to that reported by Remba et al. (1979). We have also investigated the Raman spectra of the cyanide and fluoride complexes of ferric HRP and have found that they resemble the azide and fluoride metmyoglobin complexes, respectively. As expected for Soret excitation, the principal vibrational modes observed in Figures 2 and 3 are polarized ($\rho < 0.75$) (see Table I). However, the depolarization ratios rarely achieve the $^1/_8$ value expected for D_{4h} symmetry, indicating that the effective symmetry is most likely reduced. This effect, plus the conjugation of the vinyl substituents with the porphyrin π system (Adar, 1975), contributes additional bands to the high-frequency Raman spectra of protoheme derivatives when compared to the more symmetric heme species described below.

The Soret excitation spectra are distinct from those obtained for the same compounds with α,β-band excitation, particularly in the 1550–1600-cm^{-1} region, where the structure-sensitive anomalously polarized mode (Spaulding et al., 1975) is replaced by polarized modes. Yamamoto et al. (1973) were the first to point out that these polarized modes are sensitive to spin state. For the six-coordinate myoglobin derivatives they investigated with 441.6-nm excitation, the ratio of intensities for the bands at 1566 and 1584 [I(1566)/I(1584)] increased as the high-spin content increased. The data of Figures 2 and 3 confirm this correlation and demonstrate that it also applies to six-coordinate high- and low-spin protoheme model compounds. Moreover, five-coordinate high-spin protoheme compounds show a strong polarized mode at 1574 cm^{-1}, intermediate between the 1584-cm^{-1} low-spin and 1566-cm^{-1} six-coordinate high-spin marker bands. Thus, the high-frequency polarized mode shows the same general dependence on heme structure as reported for band IV, the high-frequency ap mode: as the C_t–N distance increases from six-coordinate low-spin through five-coordinate high-spin to six-coordinate high-spin the frequency of the band decreases. However, in the case of band IV the overall decrease amounts to 30 cm^{-1}

[4] Both metmyoglobin azide and aquometmyoglobin are in spin-state equilibria at room temperature. The low-spin form is favored for the azide complex, and the high-spin form is favored for the aquo complex (Smith & Williams, 1970).

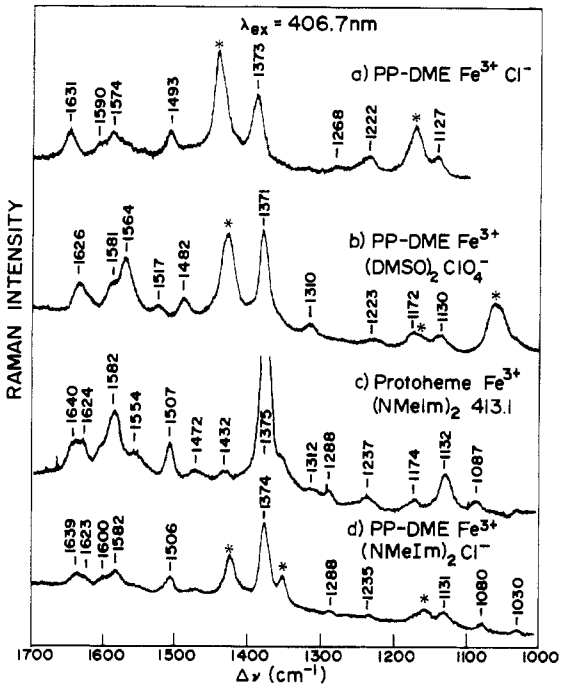

FIGURE 3: Resonance Raman spectra of several protoheme model compounds. The compounds used in (a), (b), and (d) were dissolved in methylene chloride; for the compound in (c) the aqueous solvent system described under Materials and Methods was used. Solvent- and nonresonance-enhanced ligand modes are indicated by asterisks. Instrumental conditions are as described in Figure 2.

Table I: Depolarization Ratios: Low-Spin Ferric Heme Compounds[a]

Fe^{3+}PPIXDME-$(NMeIm)_2$		Fe^{3+}OEP$(NMeIm)_2$		heme $a^{3+}(NMeIm)_2$	
band (cm^{-1})	ρ[b]	band (cm^{-1})	ρ	band (cm^{-1})	ρ
				1670	0.28 ± 0.05
1639	0.57 ± 0.05	1640	0.75 ± 0.05	1642	0.35
1623	0.43				
1582	0.42	1591	0.45	1590	0.40
1506	0.24	1507	0.26	1506	0.20
1472		1469	0.50	1474	0.51
1374	0.30	1377	0.34	1374	0.33
1288		1286	0.36	1285	0.28
1235	0.49	1230	0.46	1238	0.48
1131	0.49	1138	0.60	1132	0.60
1080	0.38	1078	0.36	1078	0.20
1030		1028	0.33	1030	0.26

[a] Excitation frequency = 406.7 nm. [b] $\rho = I_\perp/I_\parallel$.

for the heme complexes of Figures 2 and 3, whereas for the polarized mode the corresponding decrease is only 18 cm^{-1}. This observation indicates a less dramatic C_t–N distance dependence for the polarized mode. Table II summarizes the positions of the prominent bands in Figures 2 and 3 as well as vibrational frequencies observed for the same compounds with excitation in the visible region.

With α,β-band excitation a polarized mode in the 1500-cm^{-1} region is observed (band II) which is sensitive to heme iron spin and coordination. A band in the same region is also prominent in the Soret excitation Raman spectra we report and exhibits the same dependence; we conclude that band II is enhanced by both α,β and Soret laser lines. For six-coordinate high-spin derivatives band II occurs at 1482 cm^{-1} and shifts to 1496 cm^{-1} for five-coordinate high-spin species. In six-coordinate low-spin protoheme compounds the observed frequency is 1507 cm^{-1}. However, other bands are also apparent in the 1470–1510-cm^{-1} region (for example, we observe a 1472-cm^{-1} band in the six-coordinate low-spin species in Figure 3), and we have found correlations based only on band II positions to be somewhat tenuous.

In addition to the bands in the 1565–1585-cm^{-1} and 1480–1510-cm^{-1} regions, two other bands appear to be related to heme geometry in the spectra of Figures 2 and 3. Six-coordinate high-spin complexes show modes at 1396 (clearly resolved in the fluoride complexes in Figure 2 and as a shoulder in the metaquomyoglobin spectrum) and at 1515–1520 cm^{-1} which are weak or absent in the spectra of the other two classes of protoheme compounds. The latter set of bands may also be confused with band II.

Hemes with Saturated Ring Substituents. Our attempts to extrapolate the correlations developed in the previous section between protoheme structure and Raman frequencies to *c*-type cytochromes and to heme *a* containing species were only partially successful. For band II the same pattern emerges. However, for the polarized mode in the high-frequency region inconsistencies are apparent. This behavior is demonstrated for species with saturated ring substituents in Figure 4 where we have collected spectra of representative six-coordinate low-spin (parts c, e, and f), five-coordinate high-spin (a and d), and six-coordinate high-spin (part b) compounds. We have also recorded the Raman spectrum of bis(cyano)Fe^{3+}OEP and find that its vibrational properties are similar to those of the bis(NMeIm) complex; its principal high-frequency vibrations occur at 1590, 1505, and 1376 cm^{-1}. In the 1500-cm^{-1} region, the low-spin species show band II at 1507 cm^{-1}; for the high-spin compounds band II occurs at 1496 cm^{-1} for five-coordinate complexes and at 1482 cm^{-1} when the iron is six-coordinate. In the high-frequency region, there is a positive shift of ~10 cm^{-1} in frequency for the structure-sensitive polarized mode for the hemes with saturated substituents compared to the corresponding protoheme derivatives. Thus the six-coordinate low-spin indicator occurs near 1590 cm^{-1}, the five-coordinate high-spin band is at 1584 cm^{-1}, and the six-coordinate high-spin mode shows at 1575 cm^{-1}. As with the protoheme species, however, the total decrease in the frequency of the high-frequency polarized mode as the C_t–N distance increases from its six-coordinate low-spin value (1.989 Å; Collins et al., 1972) to its six-coordinate high-spin value (2.045 Å; Mashiko et al. 1978) is ~18 cm^{-1}.

Protoheme is distinct from the species in Figure 4 in that it has unsaturated substituents at two of the β-carbon positions, i.e., vinyl groups at C(2) and C(4). The Raman data above thus indicate that upon Soret excitation of iron porphyrin compounds the observed frequency of the mode in the 1560–

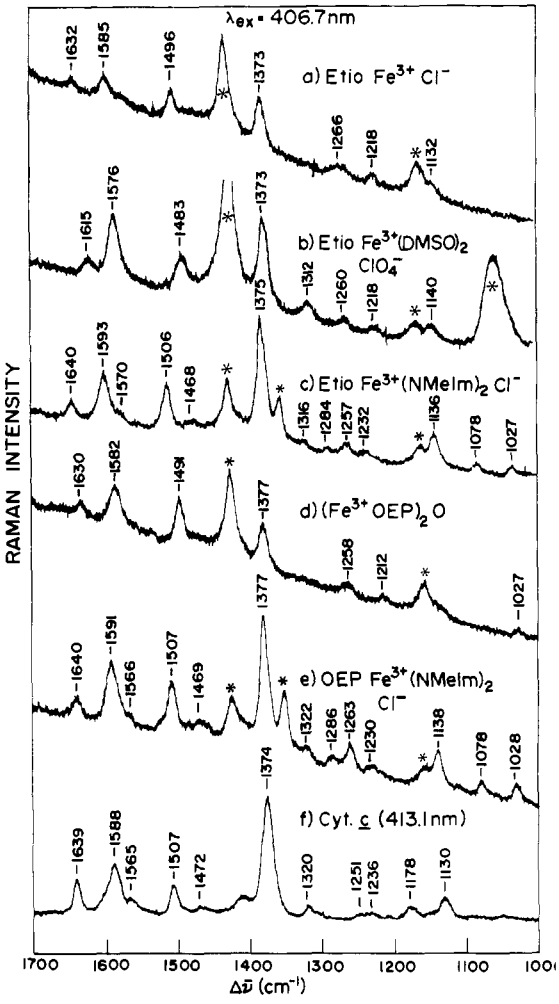

FIGURE 4: Resonance Raman spectra of several iron etioporphyrin I and octaethylporphyrin model compounds and of ferric cytochrome *c*. The model compounds were dissolved in methylene chloride; cytochrome *c* was dissolved in the aqueous buffer system described under Materials and Methods. Solvent- and nonresonance-enhanced ligand modes are indicated by asterisks. Instrumental conditions are as described in Figure 2.

1600-cm^{-1} region reflects three different structural aspects of the chromophore: (a) the spin state of the iron, (b) the coordination number of the iron, and (c) the nature of the peripheral substituents. For band IV observed with α,β-band excitation, it is apparent that the frequency position reflects only C_t–N distance, i.e., structural features a and b above, since similar values of A and K in eq 1 can be obtained from Raman data for metalloporphyrins with either saturated or unsaturated β-carbon peripheral substituents. A plausible explanation for the dichotomy in behavior of these two modes can be constructed on the basis of the normal coordinate analysis of Abe et al. (1978) and is considered in detail below.

Heme a Species. The data above demonstrate the usefulness of Soret excitation Raman data to the assignment of heme geometries provided that proper account of the pattern of peripheral substituents is taken. In heme *a* these substituents are distinct from those of protoheme and of the compounds in Figure 4 in that a hydroxyfarnesylethyl group occurs at position 2, a vinyl at ring position 4, and a formyl at ring position 8. Thus we have carried out a classification of the structure-sensitive heme *a* modes observed upon Soret excitation and show representative spectra of the various derivatives in Figure 5. Six-coordinate low-spin heme a^{3+} (Figure 5c) shows bands at 1506 and 1590 cm^{-1} which are replaced by bands at 1492 and 1581 cm^{-1} in the five-coordinate high-spin

Table II: Spin State, Coordination Geometry, and Selected Raman Frequencies for Various Hemes and Heme Proteins

Compound	Spin State	Coordination	Raman Frequencies λ_{ex} = Soret			Raman Frequencies* λ_{ex} = visible		
						p	ap	dp
A. Protoheme Species								
MetHbF	$^5/_2$	6	1482	1567	1623	1482	1555	1608
MetMbF	$^5/_2$	6	1482	1566	1622	1483	1557	1609
$MetMbH_2O$	$^5/_2$	6	1482	1565	1622	1481	1562	1611
$PP\text{-}DMEFe^{3+}(DMSO)_2$	$^5/_2$	6	1482	1564	1626	1475	1560	1610
oxidized HRP	$^5/_2$**	5	1498	1573	1630	1500	1575	1630
$PP\text{-}DMEFe^{3+}Cl^-$	$^5/_2$	5	1493	1574	1631	1495	1572	1632
$MetMbN_3^-$	$^1/_2$†	6	1506	1584	1621, 1640	----	----	----
Protoheme $Fe^{3+}(NMeIm)_2$	$^1/_2$	6	1507	1582	1624, 1640	1503	1586	1638
$PP\text{-}DMEFe^{3+}(NMeIm)_2$	$^1/_2$	6	1506	1582	1623, 1639	----	----	----
B. Hemes with all ring positions saturated								
$EtioFe^{3+}(DMSO)_2$	$^5/_2$	6	1483	1576	1615	1481	1563	1613
$EtioFe^{3+}Cl^-$	$^5/_2$	5	1496	1585	1632	1493	1568	1629
$(Fe^{3+}OEP)_2O$	$^5/_2$	5	1491	1582	1630	1494	1570	1630
$EtioFe^{3+}(NMeIm)_2$	$^1/_2$	6	1506	1593	1640	1505	1584	1641
$OEPFe^{3+}(CN^-)_2$	$^1/_2$	6	1505	1590	----	----	----	----
$OEPFe^{3+}(NMeIm)_2$	$^1/_2$	6	1507	1591	1640	1506	1587	1640
Cyt c^{3+}	$^1/_2$	6	1506	1588	1640	1502	1582	1636
C. Heme a Species††								
Heme $a^{3+}(DMSO)_2$	$^5/_2$	6	1482	1572	1615, 1672	----	----	----
Cyt a_3^{3+}	$^5/_2$	6	1478	1572	1615, 1675	----	----	----
Cyt $a_3^{3+}\cdot HCOOH$	$^5/_2$	6	1478	1572	1615, 1675	----	----	----
Heme $a^{3+}Cl^-$	$^5/_2$	5	1492	1581	1632, 1676	----	----	----
Heme $a^{3+}(NMeIm)_2$	$^1/_2$	6	1506	1590	1642, 1670	----	----	----
Cyt a^{3+}	$^1/_2$	6	1506	1590	1641, 1650	----	----	----
Cyt $a_3^{3+}\cdot CN^-$	$^1/_2$	6	1506	1590	1641, 1674	----	----	----

*From tables compiled by Sievers et al. (1979) and by Spiro et al. (1979). **The assignment of HRP as pure high spin is somewhat ambiguous: see Maltempo (1976) and also Sievers et al. (1979). †See footnote 4. ††The cytochrome *a* and a_3 assignments are made in the following paper (Babcock et al., 1981).

complex (Figure 5a). For the six-coordinate high-spin model compound (Figure 5b), these bands occur at 1482 and 1572 cm^{-1}. The band observed in the high-frequency region near 1670 cm^{-1} in these species is due to the heme *a* formyl group which is clearly resonance enhanced with Soret laser lines (Salmeen et al., 1978; Tsubaki et al., 1980). The Soret spectra differ markedly from the heme *a* spectra we have obtained with α-band excitation (Babcock et al., 1979). With λ_{ex} = 592 nm the structure-sensitive ap mode is observed and occurs at 1583 cm^{-1} for the six-coordinate low-spin species; there is no indication of either a structure-sensitive polarized mode in the 1500-cm^{-1} region or of the heme *a* carbonyl band near 1670 cm^{-1}.

Depolarization ratios for the six-coordinate low-spin heme $a^{3+}(NMeIm)_2$ are listed in Table I. The principal Raman bands in the spectra of Figures 2–5 are summarized in Table II; we have also tabulated, where possible, the structure-sensitive anomalously polarized, depolarized, and polarized modes for the same compounds when excited with laser lines in resonance with the heme Q-band transitions.

Discussion

Soret excitation Raman spectroscopy offers several advantages over the more commonly employed heme α,β-band excitation spectroscopy. These include the use of both lower heme concentrations, generally by a factor of ~10, and lower incident laser powers. In addition, polarized low-frequency modes are usually observed, and several of these reflect vibrations involving the central iron atom directly. Nagai et al. (1980) have exploited this phenomenon adroitly in their study of the iron–histidine stretching frequency in hemoglobin. Finally, in the protein cytochrome oxidase, which is our

Table III: Heme Structure Sensitive Raman Bands

mode	excitation[a] region	mode character[b] (mode number)	K_i ($cm^{-1}/Å$)[c]	A_i (Å)[c]
polarized (1480–1510 cm^{-1})	visible, Soret	C_m–C_α (ν_3)	375.5	6.01
anomalously polarized (1550–1600 cm^{-1})	visible	C_m–C_α (ν_{19})	555.6	4.86
polarized (1560–1600 cm^{-1})	Soret	C_β–C_β (ν_2)	300	7.27 (protoheme)
			300	7.30 (saturated)
			300	7.29 (heme *a*)
depolarized (1600–1650 cm^{-1})	visible (Soret)	C_m–C_α (ν_{10})	423.7	5.87

[a] Indicates heme spectral regions in which resonance enhancement of the mode is generally observed; see text for details. [b] From the normal coordinate analysis of Abe et al. (1978); the carbon–carbon bond indicated makes the major, but not sole, contribution to the specified vibration. [c] See eq 1.

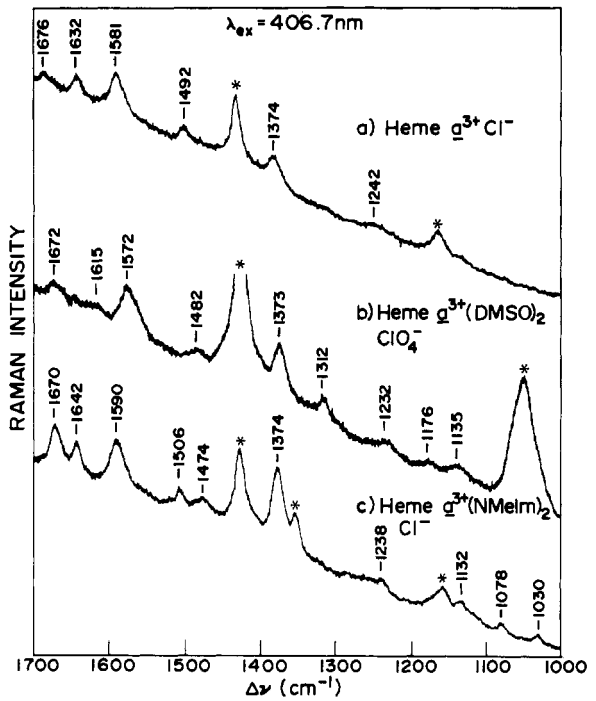

FIGURE 5: Resonance Raman spectra of several heme *a* model compounds dissolved in methylene chloride. Solvent- and nonresonance-enhanced ligand vibrations are indicated by asterisks. Instrumental conditions are as described in Figure 2.

principal focus in the following paper, Soret excitation provides the most straightforward technique by which to separate low-spin cytochrome *a* vibrations from those of high-spin cytochrome a_3 (Babcock et al., 1980). The experiments reported here provide a systematic classification of the iron porphyrin high-frequency modes observed when Soret exciting lines are used and of the structural information which can be extracted from the frequencies of these modes.

It was recognized fairly early in the application of resonance Raman spectroscopy to heme proteins that the scattering mechanism in the Soret was primarily controlled by Franck–Condon overlap factors and hence was distinct from the vibronic or Herzberg–Teller mechanism operative when Q-band excitation was employed (Nafie et al., 1973; Friedman & Hochstrasser, 1973; Spiro, 1974). Thus modes in which there is origin displacement in the excited state dominate the Raman spectrum obtained with Soret excitation, whereas anomalously polarized and depolarized modes which are active in vibronic mixing are the principal components of heme Raman spectra taken with visible laser lines. Nonetheless, two of the bands we observe routinely with Soret excitation of hemes and heme proteins, the polarized oxidation state marker band in the 1345–1380-cm^{-1} region (band I) and the polarized mode in the 1480–1510-cm^{-1} region, (band II) are also common features of visible excitation Raman spectra. The data we have presented above indicate that the correlations between spin, coordination number, and oxidation state developed for these two modes are independent of whether the excitation frequency is in resonance with the α,β- or γ-band transitions.

Two other modes, however, the ap mode in the 1550–1600-cm^{-1} region (band IV) and the dp mode in the 1600–1650-cm^{-1} region (band V), are not strongly and consistently enhanced upon Soret excitation. In the band V region, two effects appear to influence the Soret excitation spectra. For heme species with saturated β-carbon substituents, Table II shows that a good correlation exists between the frequency of the dp mode observed with visible excitation and that of the highest frequency mode in our Soret excitation Raman spectra. For a representative compound in this class, $OEPFe^{3+}(NMeIm)_2$, Table I shows that the 1640-cm^{-1} mode is depolarized, and thus we conclude that the same vibration (i.e., that which gives rise to band V) is active with both Soret and visible excitation.[5] The second effect contributing lines in the 1600–1680-cm^{-1} region is apparent when the heme *a* and protoheme derivatives are considered. For heme *a* the formyl vibration is observed at 1670–1676 cm^{-1} in aprotic solvents. Band V appears at slightly lower frequencies and shows a dependence on porphyrin core size similar to that of the heme derivatives with saturated substituents (Table II). For protoheme species the 1600–1650-cm^{-1} region is dominated by a vibration at 1621–1626 cm^{-1}; only in low-spin species is band V at 1640 cm^{-1} clearly observed. Because vinyl vibrations are expected in the 1620-cm^{-1} region, we assign the mode observed near this frequency in protoheme species as being predominantly due to the carbon–carbon double bond stretching mode.

For the polarized mode in the 1560–1600-cm^{-1} region, the data we have presented demonstrate a correlation between the observed frequency and the coordination and spin state of the heme-bound iron. In this regard it parallels the behavior of the ap mode in the same region. There are, however, quantitative differences between the two: (a) the position of the polarized mode is also a function of the porphyrin β-carbon substituents (for the ap mode this dependence does not appear to be strong) and (b) the shift in the position of band IV as the heme C_t–N distance is changed is greater than the corresponding shift in the position of the polarized mode. We have attempted to make the differences between the various structure-sensitive modes more apparent by calculating approximate K and A values from eq 1 for the polarized mode from the data we have collected and comparing these to

[5] The difference in depolarization ratio for band V in low-spin heme *a* and protoheme species under visible vs. Soret excitation reflects excitation frequency dependence in the scattering tensor. For example, for Fe^{3+}PPIX DME$(NMeIm)_2$, $\rho = 0.74$ for the 1640-cm^{-1} band when excitation is at 514.5 nm. The depolarization ratio for this mode decreases gradually to its value in Table I as the excitation frequency approaches that of the Soret band maximum (P. M. Callahan and G. T. Babcock, unpublished observations).

analogous calculations carried out for bands II, IV and V by Huong & Pommier (1977) and by Spiro et al. (1979) (Table III). The sensitivity of the 1560–1600-cm^{-1} polarized mode to β-carbon substituent is reflected in the different A values for the indicated classes of hemes; the less dramatic dependence on heme C_t–N distance is evident in the smaller value of K relative to those of the other modes.

The polarized high-frequency mode appears to have little or no dependence on the identities of the iron axial ligands, at least for the ferric oxidation state. Table II shows that for protoheme species in the low-spin state essentially identical frequencies are observed for bis(N-methylimidazole) and for histidine–azide ligand combinations. A similar insensitivity to ligand identity is apparent for the high-spin compounds. For hemes with saturated peripheral substituents a slight frequency difference is observed when bis(N-methylimidazole) and bis(cyano) compounds are compared with the histidine–methionine combination in cytochrome c. This may reflect a real axial ligand dependence or the fact that the substituents in the 2 and 4 positions on the ring periphery in cytochrome c are involved in thioether linkages.

The observations and differences described above regarding the behavior of the four structure-sensitive modes summarized in Table II can be rationalized by reference to the recent normal coordinate analysis of Abe et al. (1978). Bands II, IV, and V correspond to vibrations $\nu_3(A_{1g})$, $\nu_{19}(A_{2g})$, and $\nu_{10}(B_{1g})$, respectively, in their normal coordinate analysis, and the polarized mode we observe in the 1560–1600-cm^{-1} region with Soret excitation can be assigned as the analogue of their $\nu_2(A_{1g})$. Abe et al. (1978) have shown that ν_3, ν_{19}, and ν_{10} have considerable α-carbon–methine-carbon stretching character whereas ν_2 involves primarily β-carbon–β-carbon stretching. Consequently, the more dramatic C_t–N distance dependence of bands II, IV, and V relative to ν_2 is a manifestation of the fact that the pyrrole ring maintains a fairly rigid structure, and shifts in porphyrin geometry as a result of core expansion are accomodated largely by distortions in the α-carbon–methine-carbon–α-carbon bond angle. Substituents to the pyrrole β carbons, on the other hand, are predicted and observed to alter the frequency of ν_2 without perturbing ν_3, ν_{19}, or ν_{10} to a significant extent. In this regard, Kitagawa and co-workers (Abe et al., 1978) have shown that ν_{11}, the B_{1g} mode which represents the out of phase analogue to ν_2, is also sensitive to the nature of the β-carbon substituents.

The data we have presented above demonstrate that Soret excitation Raman spectroscopy of hemes and heme proteins can yield structural information analogous to that obtained with visible excitation. This information is, however, somewhat more difficult to extract because the frequency of the structure-sensitive modes is also a function of the nature of the peripheral substituents and because the changes in frequency upon change in structure is less dramatic than for band IV. Nonetheless, there are a number of advantages associated with Soret Raman, particularly in the less severe demands upon protein concentration and laser power. In the following paper, we present Soret excitation Raman results on cytochrome oxidase which demonstrate these and other aspects of the usefulness of Soret Raman.

Acknowledgments

We thank Professor C. K. Chang and Brian Ward for supplying several of the heme compounds used in this investigation and Dr. I. Salmeen for several useful discussions.

References

Abe, M., Kitagawa, T., & Kyogoku, Y. (1978) *J. Chem. Phys. 69*, 4526–4534.
Adar, F. (1975) *Arch. Biochem. Biophys. 170*, 644–650.
Babcock, G. T., & Salmeen, I. (1979) *Biochemistry 18*, 2493–2498.
Babcock, G. T., Vickery, L. E., & Palmer, G. (1976) *J. Biol. Chem. 251*, 7907–7919.
Babcock, G. T., Ondrias, M. R., Gobeli, D. A., Van Steelandt, J., & Leroi, G. E. (1979) *FEBS Lett. 108*, 147–151.
Babcock, G. T., Callahan, P. M., McMahon, J. J., Ondrias, M. R., & Salmeen, I. (1980) *Proc. Symp. Interact. Iron Proteins Oxygen Electron Transp.* (in press).
Babcock, G. T., Callahan, P. M., Ondrias, M. R., & Salmeen, I. (1981) *Biochemistry 20* (following paper in this issue).
Collins, D. M., Countryman, R., & Hoard, J. L. (1972) *J. Am. Chem. Soc. 94*, 2066–2072.
Dolphin, D. H., Sams, J. R., & Tsin, T. G. (1977) *Inorg. Chem. 16*, 711–717.
Felton, R. H., & Yu, N.-T. (1978) *Porphyrins 3*, 347–393.
Friedman, J. M., & Hochstrasser, R. M. (1973) *Chem. Phys. 1*, 457–467.
Huong, P. V., & Pommier, J. C. (1977) *C. R. Hebd. Seances Acad. Sci., Ser. C 285*, 519.
Kitagawa, T., Ozaki, Y., & Kyogoku, Y. (1978) *Adv. Biophys. 11*, 153–196.
Lemberg, R., Bloomfield, B., Caiger, P., & Lockwood, W. (1955) *Aust. J. Exp. Biol. Med. Sci. 33*, 435–444.
Maltempo, M. M. (1976) *Biochim. Biophys. Acta 434*, 513–518.
Mashiko, T., Kastberm, M. E., Spartalian, K., Scheidt, R. W., & Reed, C. A. (1978) *J. Am. Chem. Soc. 100*, 6354–6355.
Nafie, L. A., Pezolet, M., & Peticolas, W. L. (1973) *Chem. Phys. Lett. 20*, 563–568.
Nagai, K., Kitagawa, T., & Morimoto, H. (1980) *J. Mol. Biol. 136*, 271–289.
Ondrias, M. R., & Babcock, G. T. (1980) *Biochem. Biophys. Res. Commun. 93*, 29–35.
Remba, R. D., Champion, P. M., Fitchen, D. B., Chiang, R., & Hager, L. P. (1979) *Biochemistry 18*, 2280–2290.
Rousseau, D. L., Friedman, J. M., & Williams, P. F. (1979) *Topics Curr. Phys. 11*, 203–252.
Salmeen, I., Rimai, L., & Babcock, G. T. (1978) *Biochemistry 17*, 800–806.
Scholler, D. M., & Hoffman, B. M. (1979) *J. Am. Chem. Soc. 101*, 1655–1662.
Shelnutt, J. A., Cheung, L. D., Chang, R. C. C., Yu, N.-T., & Felton, R. H. (1977) *J. Chem. Phys. 66*, 3387–3398.
Sievers, G., Österlund, K., & Ellfolk, N. (1979) *Biochim. Biophys. Acta 581*, 1–14.
Smith, D. W., & Williams, R. J. P. (1970) *Struct. Bonding (Berlin) 7*, 1–45.
Spaulding, L. D., Chang, C. C., Yu, N.-T., & Felton, R. H. (1975) *J. Am. Chem. Soc. 97*, 2517–2525.
Spiro, T. G. (1974) *Acc. Chem. Res. 7*, 339–345.
Spiro, T. G., Stong, J. D., & Stein, P. (1979) *J. Am. Chem. Soc. 101*, 2648–2655.
Tsubaki, M., Nagai, K., & Kitagawa, T. (1980) *Biochemistry 19*, 379–385.
Yamamoto, T., Palmer, G., Gill, D., Salmeen, I., & Rimai, L. (1973) *J. Biol. Chem. 248*, 5211–5213.
Zobrist, M., & LaMar, G. N. (1978) *J. Am. Chem. Soc. 100*, 1944–1946.